

Received June 21, 2021, accepted June 29, 2021, date of publication July 1, 2021, date of current version July 9, 2021.

Digital Object Identifier 10.1109/ACCESS.2021.3094044

Multi-Objective Non-Fragile Robust Attitude Control for Flexible Microsatellite Close-Proximity Inspection

YI LI 

The Seventh Research Division and the Center for Information and Control, School of Automation Science and Electrical Engineering, Beihang University (BUAA), Beijing 100191, China

e-mail: liyi309@163.com

This work was supported by the National Natural Science Foundation of China under Grant 61520106010.


ABSTRACT In this paper, the non-fragile robust attitude control problem is investigated for flexible microsatellite close-proximity inspection, with external disturbances, parameter uncertainties and input constraints. Firstly, the attitude motion model of microsatellite with flexible appendages is established. Secondly, a non-fragile robust dynamic output feedback controller (RDOFC) with multiplicative gain variations (MGV) is designed to satisfy the multi-objective requirements, including pole assignment, H_∞ disturbances attenuation and input constraints. Based on the Lyapunov stability theory, the design of the non-fragile robust H_∞ attitude control is formulated as the linear matrix inequality (LMI) condition. Finally, numerical simulations are performed to demonstrate the effectiveness of the proposed controller.

INDEX TERMS Attitude control, non-fragile H_∞ , flexible microsatellite, multi-objective, dynamic output feedback.

I. INTRODUCTION

The capability of space target inspection in close proximity is the premise of space situational awareness and approaching operations. Due to the inherent advantages of small size and high cost-effectiveness, microsatellites are applied into several space close-proximity inspection missions, such as XSS-11 [1], MiTeX [2], and BX1 [3]. Those missions have stimulated the demand for attitude control capabilities of microsatellites, including higher pointing performance and better robustness.

In order to achieve the attitude control performance, three major problems should be considered. Firstly, the microsatellite is generally equipped with flexible appendages like large antennas and solar array, and the generated vibration will make the high-accuracy attitude control more complicated. Secondly, in practice engineering, the microsatellite suffers from external disturbances in space environments [4], and parameter uncertainties caused by the change of moment of inertia [5]. The disturbances and uncertainties will deteriorate the closed-loop stability and attitude control accuracy.

The associate editor coordinating the review of this manuscript and approving it for publication was Guangdeng Zong .

Thirdly, the attitude control input torque is limited because of the constraint of the reactor wheel output torque [6]. Besides, in order to achieve desired transient control performance, the closed-loop poles of the attitude control system (ACS) should lie in a specified disc region of the stable half-plane. Thus, the microsatellite attitude controller design is a multi-objective problem. In recent years, the problem of attitude control for flexible satellite has attracted considerable attention, and many control methods have been elaborately designed, such as fault-tolerant-based control [7]–[9], disturbance-observer-based control [10]–[13] and adaptive-backstepping-based control [14]. However, the above papers do not consider all of the mentioned problems. On the other hand, as a systematic and effective method to deal with multi-objective problem, robust H_∞ control theory has been successfully utilized into various systems [15], [16]. In [5], a mixed H_2/H_∞ attitude control design is proposed for microsatellite system with the external disturbances and parameter uncertainties considered. In [17], a robust H_∞ state feedback controller with additive gain variations (AGV) is proposed for spacecraft attitude control subject to external disturbances and parameter uncertainties. However, in [5], [17], it supposed that the relative attitude angle and

angular velocity are available. Note that in several space missions, the precise measurements of angular velocity are not always satisfied because of the absence or the failure of the gyroscopes [18]. So it is desirable to develop an output feedback methodology by using only attitude angle information.

In [19], a mixed H_2/H_∞ output feedback attitude controller with parameter uncertainties, space environmental disturbances and pole placement constraints is proposed. Based on LMI, Wu and Wen [20] propose a RDOFC for flexible satellite attitude stabilization with external disturbances and model uncertainties. Furthermore, in view of the imprecise collocation, an integrated robust H_∞ attitude controller, consisting of a feedforward component and an output feedback component, is presented to handle the multi-objective problem for flexible spacecraft [21]. However, due to the control gain parameter drifts and the deviations of the measured output caused by the sensor, the parameters in controller gain matrices may be uncertain. The small parameter perturbations of the controller gain matrices may degrade the attitude control precision or destabilize the closed-loop system [22]. Hence, it is required to propose the non-fragile RDOFC. Notice that the non-fragile control problem has been addressed by a number of papers [22]–[27], and also utilized into ACS successfully [28], [29]. Liu *et al.* [28] address the non-fragile attitude control problem for rigid spacecraft, the non-fragile RDOFC is designed with respect to the additive perturbation and multiplicative perturbation. Based on [28], the non-fragile fault tolerant attitude control problem for rigid spacecraft is investigated, and the corresponding controller is designed by conducting a stochastically intermediate observer [29]. Nevertheless, to the best of our knowledge, very few researches have been devoted to the non-fragile RDOFC design method for flexible microsatellite attitude to satisfy the multi-objective requirements, which motivate our present study. The main contributions are summarized as follows.

i). In contrast to [19], [21], a non-fragile RDOFC with MGV for the microsatellite attitude is designed to satisfy the multi-objective requirements, including flexible modes, external disturbances, parameter uncertainties, input constraints and poles assignment. Besides, compared with [30], the state-derivative-dependent uncertain term in the proposed rigid-flexible coupling model is handled directly, which can decrease the complexity of the controller design.

ii). Based on the Lyapunov stability theory, the existence conditions of admissible controller under multi-objective requirements are formulated as the nonlinear matrix inequalities (NLMIs), and the NLMIs are transformed into linear matrix inequalities (LMIs) by performing a set of changing variable process. Thus, the non-fragile controller design problem can be transformed as a convex optimization problem with LMI constraints.

iii). For the nonconvex problem caused by the coupling term in matrix inequality, compared with the two-step procedure solution performed in [25], we propose

a less conservative method by constructing a Lyapunov matrix with some structure, which makes the transformation from the NLMIs to the LMIs more easily.

The rest of this paper is organized as follows. In Section II, the attitude motion control model of microsatellite with flexible appendages is established, and the multi-objective control requirements are formulated. Based on Lyapunov theorem, a non-fragile RDOFC is proposed to achieve the multi-objective requirements in section III. Section IV illustrates the numerical simulation results. Finally, the conclusions are given.

Notations: Throughout this paper, matrix transposition and matrix inverse are represented as the superscript T and -1 , respectively; \mathbb{R}^n stands for the n -dimensional Euclidean space, and $\mathbb{R}^{n \times m}$ denote the set of all $n \times m$ real matrices; $\|\cdot\|$ refers to the Euclidean vector norm or the induced matrix 2-norm. The symmetric and negative definite real matrix X is represented as $X < 0$; An ellipsis for terms induced by symmetry in complex matrix expressions is denoted as $*$. $\mathbf{0}$ and \mathbf{I} denote zero matrix and the identity matrix with compatible dimension, respectively.

II. PROBLEM FORMULATION

A. ATTITUDE DYNAMICS OF MICROSATELLITE WITH FLEXIBLE APPENDAGES

Many different coordinate reference frames are introduced to describe the attitude control model of microsatellite with flexible appendages. One can refer to Fig. 1 for the spatial directions of different frames.

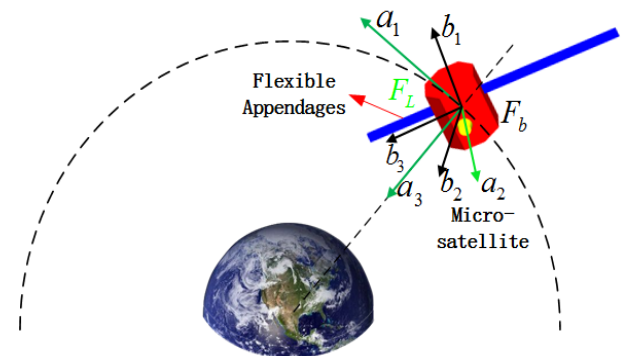


FIGURE 1. Coordinate axes of microsatellite in a circular orbit.

1) The LVLH reference frame: the frame is described by F_L , and its origin located at the mass center of microsatellite and the unit vectors (a_1, a_2, a_3) defined as a_1 along the microsatellite's velocity direction in orbit plane, a_3 toward the earth, and a_2 is completed by a right-handed Cartesian frame.

2) The body-fixed frame: the frame is described by F_b , its origin is also fixed in the mass center of the microsatellite, and three basic unit vectors (b_1, b_2, b_3) are along the inertia principal axes.

In the body reference frame F_b , the attitude dynamic equations for microsatellite with flexible appendages are

given by [31]

$$J\dot{\mathbf{w}} + F^T\ddot{\boldsymbol{\eta}} = -\mathbf{w}^\times J\mathbf{w} + \mathbf{u} + \mathbf{T}_g + \mathbf{d}$$

$$\ddot{\boldsymbol{\eta}} + C_m\dot{\boldsymbol{\eta}} + \Lambda\boldsymbol{\eta} + F\dot{\mathbf{w}} = 0, \quad (1)$$

where $J = \text{diag}(J_1, J_2, J_3)$ is the moment of inertial, $\mathbf{w} = [w_1, w_2, w_3]^T \in \mathbb{R}^3$ is the angular velocity, \mathbf{u} is the control torque acting on the microsatellite, $\mathbf{T}_g = [T_{g1}, T_{g2}, T_{g3}]^T$ donates the gravity-gradient torque presented as [32], \mathbf{d} is the external disturbances torque, $\boldsymbol{\eta}$ and F are the flexible modal coordinate and the rigid-elastic coupling matrix, respectively. $C_m = \text{diag}(2\zeta_1\omega_1, \dots, 2\zeta_N\omega_N)$ represent the modal damping matrix, with the damping ratio $\zeta_i (i = 1, \dots, N)$ and the modal frequency $\omega_i (i = 1, \dots, N)$. $\Lambda = \text{diag}(\omega_1^2, \dots, \omega_N^2)$ denotes stiffness matrix, N is the number of elastic mode.

In the motion of microsatellite, the velocity direction of microsatellite is not consistent with the thrust orientation, which results that the output of thrust cannot be used fully. Therefore, the ACS is required to achieve the space missions. In this article, the attitude of the microsatellite is described by the Euler angles. The orientation of the frame F_b relative to F_L is defined through the yaw-pitch-roll ($\psi \rightarrow \theta \rightarrow \phi$) successive rotations, and the resulting coordinate transformation is described as

$$\begin{bmatrix} \mathbf{b}_1 \\ \mathbf{b}_2 \\ \mathbf{b}_3 \end{bmatrix} = R_{bL} \begin{bmatrix} \mathbf{a}_1 \\ \mathbf{a}_2 \\ \mathbf{a}_3 \end{bmatrix}, \quad (2)$$

where

$$R_{bL} = \begin{bmatrix} c\theta c\psi & c\theta s\psi & -s\theta \\ -c\phi s\psi + s\phi s\theta c\psi & c\phi c\psi + s\phi s\theta s\psi & s\phi c\theta \\ s\phi s\psi + c\phi s\theta c\psi & -s\phi c\psi + c\phi s\theta s\psi & c\phi c\theta \end{bmatrix}$$

with $c\theta \equiv \cos\theta$, $s\theta \equiv \sin\theta$, etc. Further, the angular velocity of the reference frame F_b relative to the LVLH frame F_L can be described by

$$\mathbf{w}_{bL} = w_{bL,x}\mathbf{b}_1 + w_{bL,y}\mathbf{b}_2 + w_{bL,z}\mathbf{b}_3, \quad (3)$$

where

$$\begin{bmatrix} w_{bL,x} \\ w_{bL,y} \\ w_{bL,z} \end{bmatrix} = \begin{bmatrix} 1 & 0 & -s\theta \\ 0 & c\phi & s\phi c\theta \\ 0 & -s\phi & c\phi c\theta \end{bmatrix} \begin{bmatrix} \dot{\phi} \\ \dot{\theta} \\ \dot{\psi} \end{bmatrix}.$$

Assuming that the microsatellite motion is in a circular orbit. Then the angular velocity of the frame F_b relative to the inertial reference frame F_i is expressed as

$$\mathbf{w} = \mathbf{w}_{bi} = \mathbf{w}_{bL} + \mathbf{w}_{Li} = \mathbf{w}_{bL} - n\mathbf{a}_2 \quad (4)$$

where n represents the orbit angular rate of the microsatellite. Substituting (2) and (3) into (4), we obtain $\mathbf{w} = w_1\mathbf{b}_1 + w_2\mathbf{b}_2 + w_3\mathbf{b}_3$ in which

$$\begin{bmatrix} w_1 \\ w_2 \\ w_3 \end{bmatrix} = \begin{bmatrix} 1 & 0 & -s\theta \\ 0 & c\phi & s\phi c\theta \\ 0 & -s\phi & c\phi c\theta \end{bmatrix} \begin{bmatrix} \dot{\phi} \\ \dot{\theta} \\ \dot{\psi} \end{bmatrix} - n \begin{bmatrix} c\theta s\psi \\ s\phi s\theta s\psi + c\phi c\psi \\ c\phi s\theta s\psi - s\phi c\psi \end{bmatrix}.$$

We consider the situation that the attitude deviation from the frame F_L is small, and attitude kinematics equations

can be simplified considerably. At this point, the coordinate transformation matrix R_{bL} can be simplified as

$$R_{bL} \approx \begin{bmatrix} 1 & \psi & -\theta \\ -\psi & 1 & \phi \\ \theta & -\phi & 1 \end{bmatrix}.$$

Moreover, based on equation (3), the angular velocity of F_b relative to F_L can be simplified as

$$w_{bL,x} \approx \dot{\phi}, \quad w_{bL,y} \approx \dot{\theta}, \quad w_{bL,z} \approx \dot{\psi}.$$

Hence, from equation (4), we have

$$\begin{aligned} w_1 &= \dot{\phi} - n\psi \\ w_2 &= \dot{\theta} - n \\ w_3 &= \dot{\psi} + n\phi. \end{aligned} \quad (5)$$

For the situation of the small attitude deviation, substituting (5) into (1), and ignoring the second order small terms, the attitude motion model of microsatellite with flexible appendages are described by

$$J\ddot{\mathbf{q}} + D\dot{\mathbf{q}} + G\mathbf{q} + F^T\ddot{\boldsymbol{\eta}} = \mathbf{u} + \mathbf{d}$$

$$\ddot{\boldsymbol{\eta}} + C_m\dot{\boldsymbol{\eta}} + \Lambda\boldsymbol{\eta} + F(\ddot{\mathbf{q}} + \bar{N}\dot{\mathbf{q}}) = 0, \quad (6)$$

where $\mathbf{q} = [\phi, \theta, \psi]^T$

$$G = \begin{bmatrix} 4n^2(J_2 - J_3) & 0 & 0 \\ 0 & 3n^2(J_1 - J_3) & 0 \\ 0 & 0 & n^2(J_2 - J_1) \end{bmatrix}$$

$$D = \begin{bmatrix} 0 & 0 & -n(J_1 + J_3 - J_2) \\ 0 & 0 & 0 \\ n(J_1 + J_3 - J_2) & 0 & 0 \end{bmatrix}$$

$$\bar{N} = \begin{bmatrix} 0 & 0 & -n \\ 0 & 0 & 0 \\ n & 0 & 0 \end{bmatrix}.$$

Remark 1: The attitude model mentioned above is only valid for small angle attitude deviation. It is assumed that the attitude deviation relative to the desired attitude orientation is small. The same assumption can be seen in [5], [19]. Moreover, since the roll and yaw dynamic are coupled and affected mutually in the attitude control, the three axis attitude model (6) is relatively effective comparing with only singular-axis attitude mode considered in [33].

B. MULTI-OBJECTIVE CONTROL REQUIREMENTS

Due to the displacement deviation of payload in the space motion of the microsatellite, the principal moment of inertia will cause the perturbations, which can be described as

$$J_i = J_{i0} + \Delta J_i \delta_i \quad |\delta_i| \leq 1, \quad i = 1, 2, 3,$$

where J_{i0} is the nominal value, ΔJ_i is the known perturbation envelope of J_i , and δ_i denotes the normalized uncertainty. The matrices J , D and G with the perturbation terms can be described as

$$J = J_0 + \Delta J, \quad D = D_0 + \Delta D, \quad G = G_0 + \Delta G,$$

where

$$\begin{aligned} \Delta J &= \Xi_J \Delta_J \Gamma_J, \quad \Delta D = \Xi_D \Delta_D \Gamma_D, \quad \Delta G = \Xi_G \Delta_G \Gamma_G \\ J_0 &= \begin{bmatrix} J_{10} & 0 & 0 \\ 0 & J_{20} & 0 \\ 0 & 0 & J_{30} \end{bmatrix}, \quad \Xi_J = \begin{bmatrix} \Delta J_1 & 0 & 0 \\ 0 & \Delta J_2 & 0 \\ 0 & 0 & \Delta J_3 \end{bmatrix} \\ D_0 &= \begin{bmatrix} 0 & 0 & -n(J_{10} + J_{30} - J_{20}) \\ 0 & 0 & 0 \\ n(J_{10} + J_{30} - J_{20}) & 0 & 0 \end{bmatrix} \\ G_0 &= \begin{bmatrix} 4n^2(J_{20} - J_{30}) & 0 & 0 \\ 0 & 3n^2(J_{10} - J_{30}) & 0 \\ 0 & 0 & n^2 J_{20} - J_{10} \end{bmatrix} \\ \Delta J &= \text{diag}(\delta_1, \delta_2, \delta_3), \quad \Gamma_J = \text{diag}(1, 1, 1) \\ \Xi_D &= n \begin{bmatrix} 0 & -\Delta J_1 & 0 & -\Delta J_3 & 0 & -\Delta J_2 \\ 0 & 0 & 0 & 0 & 0 & 0 \\ \Delta J_1 & 0 & \Delta J_3 & 0 & \Delta J_2 & 0 \end{bmatrix} \\ \Gamma_D &= \begin{bmatrix} 1 & 0 & 1 & 0 & -1 & 0 \\ 0 & 0 & 0 & 0 & 0 & 0 \\ 0 & 1 & 0 & 1 & 0 & -1 \end{bmatrix}^T \\ \Delta_D &= \text{diag}(\delta_1, \delta_1, \delta_3, \delta_3, \delta_2, \delta_2) \\ \Xi_G &= n^2 \begin{bmatrix} \Delta J_2 & 0 & 0 & 0 & -4\Delta J_3 & 0 \\ 0 & 0 & 3\Delta J_1 & 3\Delta J_3 & 0 & 0 \\ 0 & \Delta J_2 & 0 & 0 & 0 & -\Delta J_1 \end{bmatrix} \\ \Gamma_G &= \begin{bmatrix} 4 & 0 & 0 & 0 & 1 & 0 \\ 0 & 0 & 1 & -1 & 0 & 0 \\ 0 & 1 & 0 & 0 & 0 & 1 \end{bmatrix}^T \\ \Delta_G &= \text{diag}(\delta_2, \delta_2, \delta_1, \delta_3, \delta_3, \delta_1). \end{aligned}$$

In view of the state vector $\mathbf{x} = [\mathbf{q}^T, \dot{\mathbf{q}}^T]^T$, the linearized attitude model of microsatellite with flexible appendages can be rewritten as

$$\begin{aligned} \dot{\mathbf{x}} + Ee(\dot{\mathbf{x}}) &= A\mathbf{x} + B_1\mathbf{u} + B_2\tilde{\mathbf{d}} \\ \mathbf{y} &= C\mathbf{x}, \end{aligned} \quad (7)$$

where

$$\begin{aligned} e(\dot{\mathbf{x}}) &= \begin{bmatrix} 0 \\ \Delta J \dot{\mathbf{x}}_2 \end{bmatrix}, \quad \|e(\dot{\mathbf{x}})\| \leq \|W_0 \dot{\mathbf{x}}\|, \quad W_0 = \begin{bmatrix} 0 & 0 \\ 0 & \Xi_J \end{bmatrix} \\ A &= A_0 + \Delta A, \quad A_0 = \begin{bmatrix} 0 & I \\ -M_0^{-1}G_0 & -M_0^{-1}(D_0 - F^T F \bar{N}) \end{bmatrix} \\ \Delta A &= L\Delta H K, \quad L = \begin{bmatrix} 0 & 0 \\ -M_0^{-1}\Xi_G & -M_0^{-1}\Xi_D \end{bmatrix} \\ E &= \begin{bmatrix} 0 & 0 \\ 0 & M_0^{-1} \end{bmatrix}, \quad M_0 = J_0 - F^T F, \quad K = \text{diag}(\Gamma_G, \Gamma_D) \\ \Delta H &= \text{diag}(\Delta_G, \Delta_D), \quad \Delta H^T \Delta H \leq I \\ B_1 &= B_2 = \begin{bmatrix} 0 \\ M_0^{-1} \end{bmatrix}, \quad C = [I \ 0] \\ \tilde{\mathbf{d}} &= F^T C_m \dot{\boldsymbol{\eta}} + F^T \Lambda \boldsymbol{\eta} + \mathbf{d}. \end{aligned}$$

Remark 2: It is noted that the uncertain term $Ee(\dot{\mathbf{x}})$ is the term on the state derivative which will be handled directly in this paper. For the ACS, in general, the parameter uncertainty

can be transformed into the parameter uncertainty in the system matrix and control input matrix by the matrix inversion operation [30]. That operation increases the complexity of the control design. Moreover, it is difficult to design the non-fragile controller due to the multiple uncertainties in the control input matrix.

For dynamic equation (7), a full order non-fragile RDOFC is designed as

$$\begin{aligned} \dot{\mathbf{x}}_f &= A_{\Delta f} \mathbf{x}_f + B_{\Delta f} \mathbf{y} \\ \mathbf{u} &= C_{\Delta f} \mathbf{x}_f, \end{aligned} \quad (8)$$

where \mathbf{x}_f is the controller state. $A_{\Delta f} = A_f + \Delta A_f$, $B_{\Delta f} = B_f + \Delta B_f$, $C_{\Delta f} = C_f + \Delta C_f$. A_f , B_f and C_f are the nominal controller gain matrices to be determined. ΔA_f , ΔB_f and ΔC_f denote the MGTV matrices resulting from the control parameter drifts and other uncertain factors, and satisfy the following hypothesis.

Assumption 1: The controller gain variations matrices ΔA_f , ΔB_f and ΔC_f are described by

$$\Delta A_f = A_f F_1, \quad \Delta B_f = B_f F_2, \quad \Delta C_f = F_3 C_f, \quad (9)$$

where

$$\begin{aligned} F_1 &= \text{diag}(\delta_{a1}, \delta_{a2}, \dots, \delta_{a6}) \quad |\delta_{ai}| \leq \delta_m \quad i = 1, \dots, 6 \\ F_2 &= \text{diag}(\delta_{b1}, \delta_{b2}, \delta_{b3}) \quad |\delta_{bi}| \leq \delta_m \quad i = 1, 2, 3 \\ F_3 &= \text{diag}(\delta_{c1}, \delta_{c2}, \delta_{c3}) \quad |\delta_{ci}| \leq \delta_m \quad i = 1, 2, 3. \end{aligned}$$

Remark 3: In assumption 1, ΔA_f means that the identical relative percentage drift δ_{ai} from the nominal entries of every column of A_f is admissible, and so to ΔB_f . In practice, ΔB_f and ΔC_f are described to the degradation of sensors and actuators [34]. ΔA_f can be used to describe the errors due to the controller state error [23].

Combining system (7) and non-fragile RDOFC (8), we obtain the closed-loop system

$$\begin{aligned} \dot{\boldsymbol{\xi}} &= \tilde{A}\boldsymbol{\xi} + \tilde{B}\tilde{\mathbf{d}} - \tilde{E}e(\dot{\mathbf{x}}) \\ \mathbf{y} &= \tilde{C}\boldsymbol{\xi}, \end{aligned} \quad (10)$$

where

$$\begin{aligned} \boldsymbol{\xi} &= \begin{bmatrix} \mathbf{x} \\ \mathbf{x}_f \end{bmatrix}, \quad \|e(\dot{\mathbf{x}})\| \leq \|W_0 \dot{\mathbf{x}}\| = \|\bar{W}_0 \dot{\boldsymbol{\xi}}\| \\ \bar{W}_0 &= [W_0 \ 0], \quad \tilde{A} = \begin{bmatrix} A & B_1 C_{\Delta f} \\ B_{\Delta f} C & A_{\Delta f} \end{bmatrix} \\ \tilde{B} &= \begin{bmatrix} B_2 \\ 0 \end{bmatrix}, \quad \tilde{E} = \begin{bmatrix} E \\ 0 \end{bmatrix}, \quad \tilde{C} = [C \ 0]. \end{aligned}$$

Therefore, we can write the actual control input as

$$\mathbf{u} = C_{\Delta f} \mathbf{x}_f = \begin{bmatrix} 0 & C_{\Delta f} \end{bmatrix} \begin{bmatrix} \mathbf{x} \\ \mathbf{x}_f \end{bmatrix} = \tilde{K}\boldsymbol{\xi}. \quad (11)$$

Our goal is to design a non-fragile RDOFC (8) such that the closed-loop system (10) satisfies the following requirements.

- 1) All the closed-loop poles lie in a prescribed the disk region $D(a, b)$ (centered in $-a + j0$ with the radius $b(b < a)$).

C_f and

$$A_f = N^{-1}F_a, \quad B_f = N^{-1}F_b. \quad (14)$$

Proof: Based on Lemma 3, system (10) satisfies the requirements (1) – (2) if the matrix inequality (12) are satisfied. Define

$$P = \begin{bmatrix} Y & N \\ N & -N \end{bmatrix}, \quad \Gamma_1 = \begin{bmatrix} I & I \\ I & 0 \end{bmatrix}$$

$$\Gamma_1^T P \Gamma_1 = \begin{bmatrix} S & S \\ S & Y \end{bmatrix}$$

where $S = Y + N$. Then, based on the Schur Complement Formula, it is obvious that $P > 0$ is equivalent to $S > 0$ and $N < 0$. Post- and pre-multiplying (12) by $diag(\Gamma_1, I, I, I, I, \Gamma_1)$ and its transpose, respectively, can yield

$$\begin{bmatrix} (1, 1) & (1, 2) & (1, 3) & \psi_{14} & \psi_{15} \\ * & -\lambda^2 I & 0 & -\lambda E^T W_0^T & 0 \\ * & * & -\gamma^2 I & \lambda B_2^T W_0^T & 0 \\ * & * & * & -I & 0 \\ * & * & * & * & (5, 5) \end{bmatrix} < 0 \quad (15)$$

where (1, 1), (1, 2), (1, 3), (5, 5) are defined in (13),

$$\psi_{14} = \begin{bmatrix} \lambda A^T W_0^T + \lambda C_{\Delta f}^T B_1^T W_0^T \\ \lambda A^T W_0^T \end{bmatrix}$$

$$\psi_{15} = \begin{bmatrix} A^T S + C_{\Delta f}^T B_1^T S + aS \\ A^T S + aS \\ A^T Y + C^T B_{\Delta f}^T N + C_{\Delta f}^T B_1^T Y + A_{\Delta f}^T N + aS \\ A^T Y + C^T B_{\Delta f}^T N + aY \end{bmatrix}.$$

Further, the matrix inequality (15) can be rewritten as

$$Q_1 + \begin{bmatrix} \bar{M}_1 \\ 0 \end{bmatrix} \Delta H [0 \bar{N}_1] + \begin{bmatrix} 0 \\ \bar{N}_1^T \end{bmatrix} \Delta H^T [\bar{M}_1^T 0] + \begin{bmatrix} \bar{M}_2 \\ 0 \end{bmatrix} \tilde{F} [0 \bar{N}_2] + \begin{bmatrix} 0 \\ \bar{N}_2^T \end{bmatrix} \tilde{F}^T [\bar{M}_2^T 0] \leq 0, \quad (16)$$

where

$$Q_1 = \begin{bmatrix} (1, 1) & (1, 2) & (1, 3) & \hat{\psi}_{14} & \hat{\psi}_{15} \\ * & -\lambda^2 I & 0 & -\lambda E^T W_0^T & 0 \\ * & * & -\gamma^2 I & \lambda B_2^T W_0^T & 0 \\ * & * & * & -I & 0 \\ * & * & * & * & (5, 5) \end{bmatrix}$$

$$\hat{\psi}_{14} = \begin{bmatrix} \lambda A_0^T W_0^T + \lambda C_f^T B_1^T W_0^T \\ \lambda A_0^T W_0^T \end{bmatrix}$$

$$\hat{\psi}_{15} = \begin{bmatrix} A_0^T S + C_f^T B_1^T S + aS \\ A_0^T S + aS \\ A_0^T Y + C^T B_f^T N + C_f^T B_1^T Y + A_f^T N + aS \\ A_0^T Y + C^T B_f^T N + aY \end{bmatrix}$$

$$\bar{M}_1 = \begin{bmatrix} K^T \\ K^T \end{bmatrix}, \quad \bar{M}_2 = \begin{bmatrix} I & C^T & C_f^T \\ 0 & C^T & 0 \end{bmatrix}$$

$$\bar{N}_1 = [\lambda L^T W_0^T \quad L^T S \quad L^T Y]$$

$$\bar{N}_2 = \begin{bmatrix} 0 & 0 & A_f^T N \\ 0 & 0 & B_f^T N \\ \lambda B_1^T W_0^T & B_1^T S & B_1^T Y \end{bmatrix}$$

$$\tilde{F} = diag(F_1^T, F_2^T, F_3^T), \quad \tilde{F}^T \tilde{F} \leq \delta_m^2 I.$$

It follows from Lemma 1 that (16) is equivalent to the matrix inequality (13). \square

Note that the matrix inequality (13) is not a LMI due to the coupling term $C_f^T B_1^T (S - N)$ in (1, 5). To solve the problem, a two-step procedure method is proposed in [25], which is assumed that the controller gain matrix C_f is prior given, and the actual controller gain matrix C_f will be designed later. However, the two-step procedure with given matrix C_f will cause more conservatism due to the reduction in the freedom variable. Based on Lemma 2, the less conservative method which solves the problem of the existence of the coupling term is proposed in the following Theorem.

Theorem 2: Consider a disk $D(a, b)$ and positive scalars $\varepsilon_1, \varepsilon_2, \lambda, \lambda_1, \gamma, \delta_m$, system (10) satisfies the requirements (1) – (2) with the proposed non-fragile RDOFC (8) if there exist matrices $S > 0, N < 0, F_a, F_b, C_f$ such that the following LMI holds.

$$\begin{bmatrix} \Xi & \lambda_1^{-1} \Phi + \lambda_1 \Psi \\ * & -2I \end{bmatrix} < 0, \quad (17)$$

where

$$\Xi = \begin{bmatrix} (1, 1) & (1, 2) & (1, 3) & (1, 4) \\ * & -\lambda^2 I & 0 & -\lambda E^T W_0^T \\ * & * & -\gamma^2 I & \lambda B_2^T W_0^T \\ * & * & * & -I \\ * & * & * & * \\ * & * & * & * \\ * & * & * & * \\ * & * & * & * \\ * & * & * & * \\ * & * & * & * \\ \tilde{\psi}_{15} & (1, 6) & 0 & \varepsilon_2 \psi_3 & 0 \\ 0 & 0 & 0 & 0 & 0 \\ 0 & 0 & 0 & 0 & 0 \\ 0 & 0 & \psi_1 & 0 & \psi_4 \\ (5, 5) & 0 & \psi_2 & 0 & \psi_5 \\ * & -\varepsilon_1 I & 0 & 0 & 0 \\ * & * & -\varepsilon_1 I & 0 & 0 \\ * & * & * & -\varepsilon_2 I & 0 \\ * & * & * & * & -\varepsilon_2 I \end{bmatrix}$$

$$\tilde{\psi}_{15} = \begin{bmatrix} A_0^T S + aS & A_0^T (S - N) + C^T F_b^T + F_a^T + aS \\ A_0^T S + aS & A_0^T (S - N) + C^T F_b^T + a(S - N) \end{bmatrix}$$

$$\Phi = [[C_f \ 0] \ 0 \ 0 \ 0 \ 0 \ 0 \ 0 \ 0 \ 0]^T$$

$$\Psi = [0 \ 0 \ 0 \ 0 \ [B_1^T S \ B_1^T (S - N)] \ 0 \ 0 \ 0 \ 0]^T$$

with (1, 1), (1, 2), (1, 3), (1, 4), (1, 6), (5, 5), $\psi_1, \psi_2, \psi_3, \psi_4, \psi_5$ are defined as in Theorem 1. Thus, the desired nominal non-fragile RDOFC can be obtained by C_f and equation (14).

Proof: By Lemma 2 and the Schur Complement Formula, if the LMI (17) holds, then we have

$$\Xi + \Phi \Psi^T + \Psi \Phi^T < 0. \quad (18)$$

It can be easily verified that the inequality (17) is equivalent to the inequality (13). Thus, based on Theorem 2, the closed-loop system (10) satisfies the requirements (1) – (2) if the LMI (17) holds. \square

Lemma 4: Consider system (10) with the non-fragile controller given in (8), it is assumed that the initial state $\xi(0) = \begin{bmatrix} \mathbf{x}(0) \\ 0 \end{bmatrix}$ is known. With the matrices $S > 0, N < 0$ and C_f presented in Theorem 1, then the input constraint $\|u\| \leq u_{max}$ can be satisfied if there exist scalars $\vartheta > 0$ and $\varepsilon_3 > 0$ such that

$$\begin{bmatrix} -u_{max}^2 I + \varepsilon_3 \delta_m^2 I & -C_f & 0 & 0 \\ * & -\frac{1}{\vartheta} S & -\frac{1}{\vartheta} S & C_f^T \\ * & * & -\frac{1}{\vartheta} (S - N) & 0 \\ * & * & * & -\varepsilon_3 I \end{bmatrix} \leq 0 \quad (19)$$

$$\begin{bmatrix} -\vartheta I & -\mathbf{x}^T(0) & -\mathbf{x}^T(0) \\ * & -S & -S \\ * & * & -(S - N) \end{bmatrix} \leq 0. \quad (20)$$

Proof: See Appendix B. \square

Theorem 3: Consider a disk $D(a, b)$, initial state $\xi(0)$ and positive scalars $\varepsilon_1, \varepsilon_2, \varepsilon_3, \lambda, \lambda_1, \gamma, \delta_m$, the closed-loop system (10) with non-fragile RDOFC (8) satisfies the requirements (1) – (3) if there exist matrices $S > 0, N < 0, F_a, F_b, C_f$ such that the LMIs (17), (19) and (20) are satisfied.

Proof: Based on the results of Theorem 2 and Lemma 4, if there exists a feasible solution $S > 0, N < 0, F_a, F_b, C_f$ such that the matrix inequalities (17), (19) and (20) are satisfied, the non-fragile RDOFC can be obtained such that the closed-loop system satisfies the poles, H_∞ norm and input constraint requirements. \square

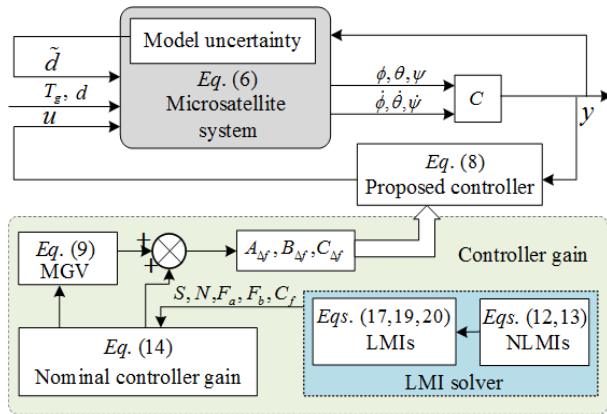


FIGURE 2. Block diagram of the non-fragile RDOFC.

As a summary, the matrix inequalities (17), (19) and (20) are the LMIs about the matrices $S > 0, N < 0, F_a, F_b, C_f$, which can be solved efficiently by convex optimization using the LMI tool [38]. Therefore, by solving the matrix inequalities (17), (19) and (20), we can obtain the feasible solution of the matrices $S > 0, N < 0, F_a, F_b, C_f$, and the desired nominal non-fragile dynamic output feedback gain matrix $A_f = N^{-1}F_a$ and $B_f = N^{-1}F_b$ can be computed easily, the control logical diagram of the whole system is illustrated in Fig. 2.

Remark 5: In [24], [36], the non-fragile output feedback control problems with AGV have been investigated.

However, for MGV in the output feedback controller, there are few results in the existing literatures. Compared with AGV, MGV is more consisted with the factual situation, which can be seen in Remark 3. Moreover, For MGV, $\Delta A_f, \Delta B_f$ and ΔC_f in the output feedback controller (8), it is difficult to transform the NLMI (13) into LMI using changing variable method [39], [40], which results that the LMI approach cannot be used and the non-fragile dynamic output feedback controller cannot be found. Based on Lemma 2, the less conservative and simpler method is proposed than the results in [25], which can transform the NLMI into LMI successfully.

IV. SIMULATION RESULTS

In this section, math simulation about attitude control for microsatellite with flexible appendages is presented to verify the stability and performance of the non-fragile RDOFC. The microsatellite is moving along a geosynchronous orbit of radius 42241 km with an orbital period of 24 h. Thus, the orbital rate microsatellite can be computed as $n = 7.2722 \times 10^{-5} rad/s$. The initial conditions and microsatellite main parameters referred to [19], [31] is summarized in Table 1.

TABLE 1. System parameters and initial condition.

Parameters	values
Mass of the microsatellite	$m = 30kg$
Nominal inertia matrix of the microsatellite	$J_0 = \text{diag}(25.3868, 24.3483, 20.3781)kgm^2$
Rigid-elastic coupling matrix	$F = \begin{bmatrix} -0.4733 & 0.4855 & 1.0140 \\ 0.5519 & 0.5503 & 1.9974 \\ -0.1530 & 0.7138 & -0.0002 \end{bmatrix}$
Modal frequency	$\varpi_1 = 0.7400, \varpi_2 = 0.7500$ $\varpi_3 = 0.7600, \varpi_4 = 0.7600$
Damping ratio	$\zeta_1 = 0.004, \zeta_2 = 0.005$ $\zeta_3 = 0.064, \zeta_4 = 0.008$
Perturbation envelops of the principal moment of inertia	$\Delta J_1 = 0.05J_{10}, \Delta J_2 = -0.05J_{20}$ $\Delta J_3 = 0.05J_{30}$
External disturbances	$d = \begin{bmatrix} 1.5 \times 10^{-5} J_1 (3\cos nt + 1) \\ 1.5 \times 10^{-5} J_2 (1.5\sin nt + 3\cos nt) \\ 1.5 \times 10^{-5} J_3 (3\sin nt + 1) \end{bmatrix}$
Perturbation terms of controller gain variation and upper bound	$\delta_{ai} = \delta_{bi} = \delta_{ci} = 0.05\sin(2\pi t)$ $\delta_m = 0.05$
Initial values of attitude angle	$\phi(0) = 0.05rad, \theta(0) = 0.03rad$ $\psi(0) = -0.05rad$
Initial values of attitude angular velocity	$\dot{\phi}(0) = 0.001rad/s$ $\dot{\theta}(0) = -0.001rad/s$ $\dot{\psi}(0) = 0.0015rad/s$
Maximum output torque	$u_{max} = 2Nm$
H_∞ performance index	$\gamma = 10$
Control parameters	$\varepsilon_1 = 0.1, \varepsilon_2 = 10, \varepsilon_3 = 100$ $\vartheta = 20, \lambda = 1, \lambda_1 = 100$

The following multi-objective requirements are satisfied with the proposed non-fragile dynamic output feedback controller (8):

- (1) All the closed-loop poles lie within a disk region $D(1.01, 1)$;
- (2) The closed-loop system is stable, and the closed-loop transfer function $\|T_{y\tilde{d}}\| < \gamma$;
- (3) The control input $\|u\| \leq u_{max}$.

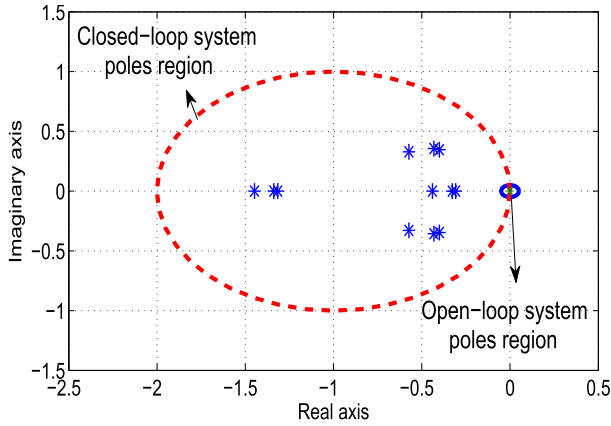


FIGURE 3. Poles of the open-loop and closed-loop system.

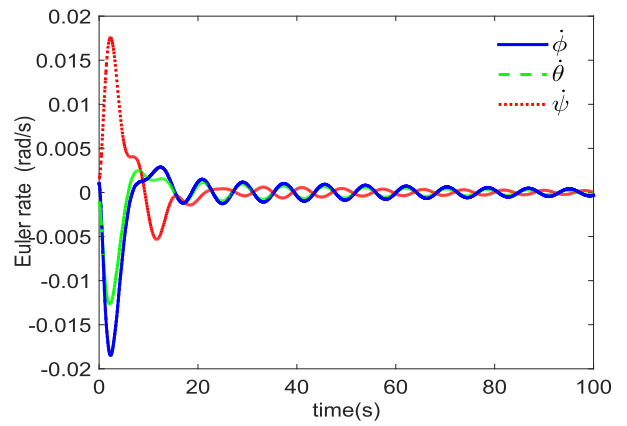


FIGURE 5. The transition processes of the euler rate.

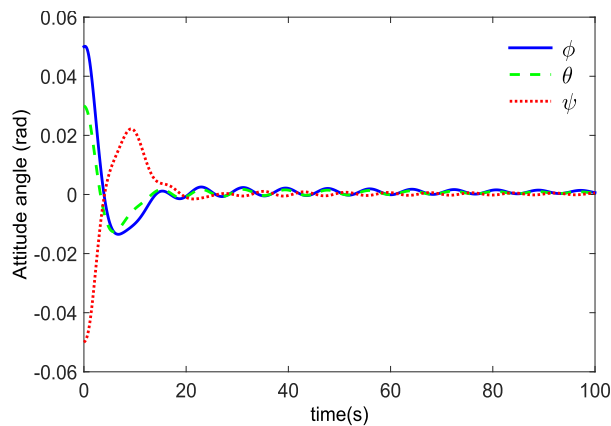


FIGURE 4. The transition processes of the euler angle.

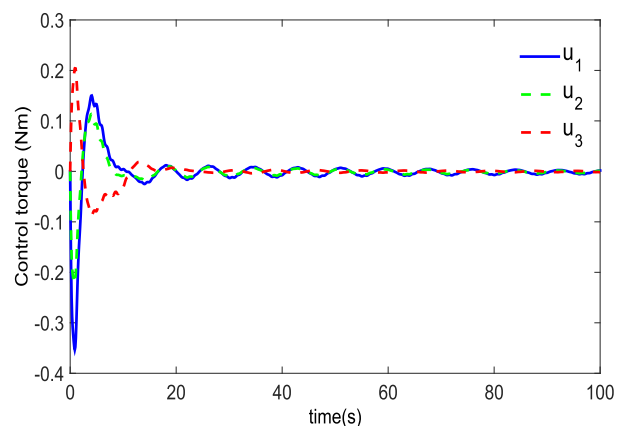


FIGURE 6. The required control torque u .

We consider the closed-loop system (10) with the non-fragile RDOFC (8). With H_∞ performance index and the system control parameters as shown in Table 1, the associated matrices $S > 0, N < 0, F_a, F_b, C_f$ can be obtained by solving the LMIs (17), (19), (20). The gain matrices A_f, B_f, C_f in the non-fragile RDOFC (8) can be obtained, as shown at the bottom of the page.

The poles placement of the open-loop system (7) and the closed-loop system (10) in the complex plane are presented in Fig. 3. It can be seen that all open-loop poles are near the origin, among which are located in the right half plane. It is

illustrated that the open-loop system (7) is unstable. With the proposed non-fragile RDOFC (8), all the closed-loop poles lie in a prescribed disk region $D(1.01, 1)$. So the requirement of poles placement is satisfied by the designed controller.

With the proposed non-fragile RDOFC (8), the Euler angle and Euler rate for microsatellite with flexible appendages are shown in Fig. 4 and Fig. 5. It demonstrates that the Euler angle and Euler rate converge to a small set containing the origin even though in the presence of the multiple perturbations including the parameter uncertainties, external disturbances, flexible mode and the controller gain variations. The required

$$A_f = \begin{bmatrix} -1.7436 & -0.0414 & -0.0345 & 0.8259 & 0.0045 & 0.0355 \\ -0.0391 & -1.7468 & -0.0378 & -0.0109 & 0.8404 & 0.0395 \\ -0.0266 & -0.0322 & -1.7870 & -0.0223 & -0.0031 & 0.9072 \\ -0.9915 & -0.0835 & -0.0603 & -0.9275 & -0.1709 & -0.0419 \\ -0.0860 & -0.9930 & -0.0663 & -0.2251 & -0.9062 & -0.0577 \\ -0.0734 & -0.0767 & -1.0442 & -0.2533 & -0.2149 & -0.8746 \end{bmatrix}, B_f = \begin{bmatrix} 1.7617 & 0.0464 & 0.0453 \\ 0.0404 & 1.7653 & 0.0466 \\ 0.0230 & 0.0302 & 1.8053 \\ 0.8236 & 0.0514 & 0.0508 \\ 0.0430 & 0.8235 & 0.0485 \\ 0.0193 & 0.0252 & 0.8477 \end{bmatrix}$$

$$C_f = \begin{bmatrix} -4.4942 & -0.8019 & -0.2853 & -20.9548 & -3.4785 & -0.8402 \\ -0.8950 & -4.1983 & -0.2066 & -3.96817 & -19.1590 & -0.2567 \\ -0.6417 & -0.4734 & -3.2429 & -2.6142 & -1.5703 & -12.9845 \end{bmatrix}.$$

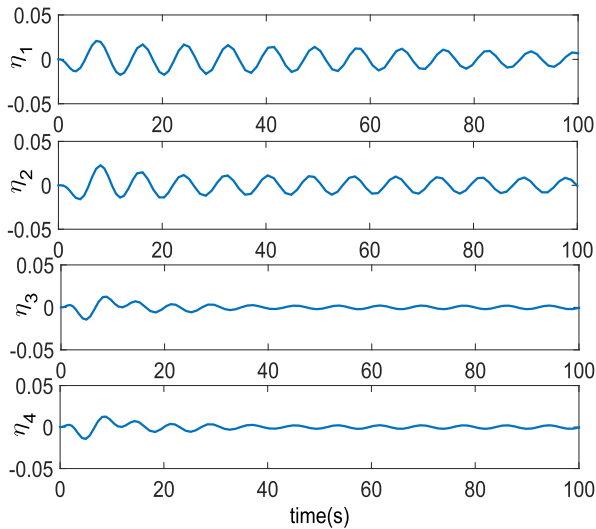


FIGURE 7. The flexible modal coordinate.

control torque is depicted in Fig. 6. We can see that the largest required control torque is below the upper bound of the output torque generated by reaction wheels. So the requirement (2) and (3) can be satisfied. Meanwhile, the modal displacements are illustrated in Fig. 7, which shows that the vibration of the flexible appendage is suppressed effectively.

In addition, to highlight the performance of the proposed non-fragile RDOFC (8), we compare it with the existing robust controller given in [39]. Considering the flexible microsatellite system (6) and the same H_∞ performance index, we obtain the following gain matrices A_f , B_f , C_f , as shown at the bottom of the page.

In such a case, each of the elements of the parameter perturbation terms F_1 , F_2 and F_3 are random numbers belonging to a uniform distribution on the interval (0,1). The responses curves of three Euler angles under the proposed non-fragile RDOFC (8) and robust controller given in [39] are shown in Figs. 8 and 9, respectively. Compared with the results in Figs. 8 and 9, we can observe that the proposed non-fragile RDOFC (8) guarantees that the Euler angles converge into a smaller convergent region than the robust controller in [39]. It is illustrated that the proposed non-fragile RDOFC (8) has better robustness performance and can achieve high control accuracy in the presence of the gain parameter perturbations.

$$A_f = \begin{bmatrix} -1.6216 & 0.0001 & -0.0003 & -7.0776 & 1.1269 & -0.2834 \\ 0.0001 & -1.624 & -0.0003 & 1.0201 & 7.1427 & -0.2254 \\ -0.0007 & -0.0005 & -1.6480 & -0.0807 & 0.0960 & 8.0078 \\ 0.2101 & -0.0314 & 0.0037 & -1.9273 & 0.0111 & -0.0197 \\ -0.0318 & -0.2089 & -0.0042 & 0.0108 & -1.9315 & 0.0198 \\ 0.0052 & 0.0043 & -0.2013 & -0.0141 & 0.0147 & -1.9813 \end{bmatrix}, B_f = \begin{bmatrix} 22.7536 & 0.9123 & -1.5473 \\ -1.2782 & 22.4673 & -4.4155 \\ -1.2252 & -4.4756 & -23.0957 \\ -16.0443 & 1.6823 & 0.8288 \\ 1.5634 & 15.5300 & -3.4306 \\ -1.2205 & -3.1685 & -14.1571 \end{bmatrix}$$

$$C_f = \begin{bmatrix} 0.5574 & -0.0326 & -0.0189 & 4.7734 & -0.4647 & 0.3537 \\ 0.0196 & 0.5218 & -0.06889 & -0.4881 & -4.5021 & 0.8142 \\ -0.0370 & -0.1017 & -0.3530 & -0.2292 & 0.9723 & 3.4230 \end{bmatrix}.$$

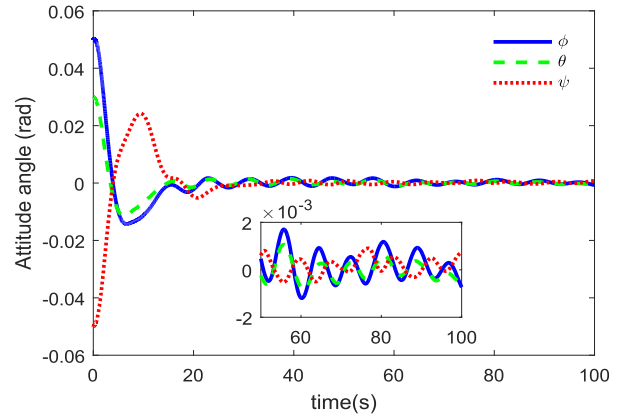


FIGURE 8. The transition processes of the euler angle under the proposed controller with uniformly distributed gain perturbation.

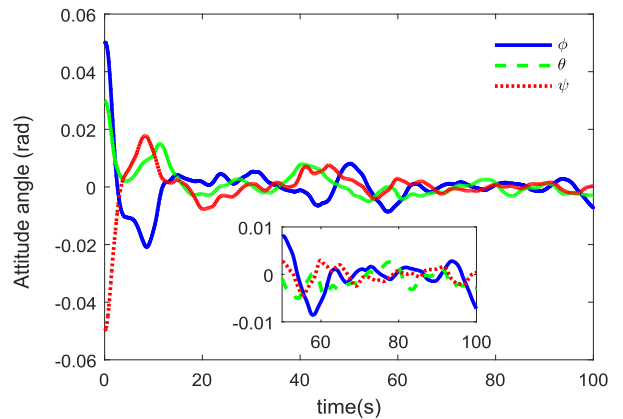


FIGURE 9. The transition processes of the euler angle under the robust controller in [39] with uniformly distributed gain perturbation.

V. CONCLUSION

In this article, we have proposed a non-fragile RDOFC with the MGV for flexible microsatellite close-proximity inspection mission in presence of flexible mode, parameter uncertainties and external disturbances. The controller is successful to satisfy the multi-objective requirements simultaneously, including poles assignment, H_∞ norm and input constraint. On the basis of the Lyapunov stability theory and LMI technique, the multi-objective attitude control problem for the microsatellite is reduced to a convex optimization problem,

and the desired non-fragile RDOFC can be obtained by solving the LMIs constraints. The final simulation results verify the high-accuracy and good robustness of the proposed controller.

APPENDIX I. PROOF OF LEMMA 3

Suppose that there exists a solution $P > 0$ satisfying the matrix inequality (12). Based on the Schur complement, then we have

$$(\tilde{A} + aI)^T \frac{P}{a} (\tilde{A} + aI) - \frac{b^2}{a} P < 0. \tag{A.1}$$

Based on the Lyapunov stability theory, it is concluded that $\sigma(\tilde{A}) \in D(a, b)$. Therefore, system (10) satisfies the requirement (1). Further, Let us consider the following Lyapunov function

$$V(\xi) = \xi^T P \xi + \int_0^T \lambda^2 \|\tilde{W}_0 \dot{\xi}\|^2 - \lambda^2 \|e(\dot{x})\|^2 d\tau. \tag{A.2}$$

Calculating the time derivative of $V(\xi)$ along the trajectory of system (10), we have

$$\begin{aligned} \Psi &= \dot{V}(\xi) + y^T y - \gamma^2 \tilde{d}^T \tilde{d} \\ &= (\tilde{A}\xi + \tilde{B}\tilde{d} - \tilde{E}e)^T P \xi + \xi^T P (\tilde{A}\xi + \tilde{B}\tilde{d} - \tilde{E}e) \\ &\quad + \xi^T \tilde{C}^T \tilde{C} \xi + \lambda^2 \|\tilde{W}_0(\tilde{A}\xi + \tilde{B}\tilde{d} - \tilde{E}e)\|^2 \\ &\quad - \lambda^2 \|e(\dot{x})\|^2 - \gamma^2 \tilde{d}^T \tilde{d} \\ &= \xi^T (\tilde{A}^T P + P \tilde{A} + \lambda^2 \tilde{A}^T \tilde{W}_0^T \tilde{W}_0 \tilde{A} + \tilde{C}^T \tilde{C}) \xi \\ &\quad - (\xi^T P \tilde{E} e + \lambda^2 \xi \tilde{A}^T \tilde{W}_0^T \tilde{W}_0 \tilde{E} e) \\ &\quad - (\xi^T P \tilde{E} e + \lambda^2 \xi \tilde{A}^T \tilde{W}_0^T \tilde{W}_0 \tilde{E} e)^T \\ &\quad + (\xi^T P \tilde{B} \tilde{d} + \lambda^2 \xi \tilde{A}^T \tilde{W}_0^T \tilde{W}_0 \tilde{B} \tilde{d}) \\ &\quad + (\xi^T P \tilde{B} \tilde{d} + \lambda^2 \xi \tilde{A}^T \tilde{W}_0^T \tilde{W}_0 \tilde{B} \tilde{d})^T \\ &\quad + \lambda^2 e^T (\tilde{E}^T \tilde{W}_0^T \tilde{W}_0 \tilde{E} - I) e \\ &\quad - 2\lambda^2 e^T \tilde{E}^T \tilde{W}_0^T \tilde{W}_0 \tilde{B} \tilde{d} \\ &\quad + \tilde{d}^T (\lambda^2 \tilde{B}^T \tilde{W}_0^T \tilde{W}_0 \tilde{B} - \gamma^2 I) \tilde{d} \\ &= \bar{M} \Phi_1 \bar{M}^T, \end{aligned} \tag{A.3}$$

where $\bar{M} = \begin{bmatrix} \xi^T & e^T & \tilde{d}^T \end{bmatrix}$, Φ_1 satisfies (A.4), as shown at the bottom of the page.

On the other hand, the matrix inequality (12) can be rewritten as (A.5), as shown at the bottom of the page.

The inequality (A.5) implies that $\Phi_1 < 0$. Based on the Lyapunov stability theory, system (10) is asymptotically stable (when $\tilde{d} = 0$). Moreover, integrating both sides of (A.3)

from zero to infinity, we have $\int_0^\infty y^T y d\tau < \int_0^\infty \gamma^2 \tilde{d}^T \tilde{d} d\tau$, which implies that $\|T_{y\tilde{d}}\| < \gamma$. Hence, the closed-loop system (10) satisfies the requirement (2). This completes the proof.

APPENDIX II. PROOF OF LEMMA 4

Consider the Lyapunov function candidate $U(\xi) = \xi^T P \xi$, which has the same Lyapunov matrix P as Lemma 3, and satisfies

$$U(\xi) \leq \vartheta,$$

where ϑ is a positive scalar. Define the ellipsoid $\Pi(P, \vartheta) = \{\xi | \xi^T P \xi \leq \vartheta\}$. For input constraint $\|u\| \leq u_{max}$, substituting the control input (11), another ellipsoid $\Pi(\tilde{K}) = \{\xi | \tilde{K}^T \tilde{K} \xi \leq u_{max}^2\}$ is presented, where the input constraint can be satisfied. Hence, the input constraint can be ensured by

$$\Pi(P, \vartheta) \subset \Pi(\tilde{K}). \tag{B.1}$$

According to [39], it is concluded that (B.1) can be guaranteed if and only if the following matrix inequality is satisfied

$$\begin{bmatrix} -u_{max}^2 I & -\tilde{K} \\ * & -\frac{1}{\vartheta} P \end{bmatrix} \leq 0. \tag{B.2}$$

Post- and pre-multiplying (B.2) by the matrix $diag(I, \Gamma_1)$ and its transpose, respectively, the inequality (B.2) can be transformed as

$$\begin{bmatrix} -u_{max}^2 I - C_{\Delta f} & 0 \\ * & -\frac{1}{\vartheta} S \\ * & * & -\frac{1}{\vartheta} (S - N) \end{bmatrix} \leq 0. \tag{B.3}$$

Denote

$$Q_2 = \begin{bmatrix} -u_{max}^2 I - C_f & 0 \\ * & -\frac{1}{\vartheta} S \\ * & * & -\frac{1}{\vartheta} (S - N) \end{bmatrix}.$$

Based on Assumption 1 about the uncertain term in the control gain matrix $C_{\Delta f}$, then (B.3) can be written as

$$Q_2 + \begin{bmatrix} I \\ 0 \\ 0 \end{bmatrix} F_3 \begin{bmatrix} 0 & C_f & 0 \end{bmatrix} + \begin{bmatrix} 0 \\ C_f^T \\ 0 \end{bmatrix} F_3^T \begin{bmatrix} I & 0 & 0 \end{bmatrix} \leq 0. \tag{B.4}$$

It follows from Lemma 1 that (B.4) is equivalent to (19).

On the other hand, for P introduced by Lemma 3, it is guaranteed that $\dot{U}(\xi) < 0$ is satisfied. Then we have $\xi^T P \dot{\xi} \leq \xi^T(0) P \dot{\xi}(0)$ for $\forall t > 0$. Thus, the condition $\xi^T P \xi \leq \vartheta$ can be guaranteed by $\xi^T(0) P \xi(0) \leq \vartheta$, which can be written as

$$\begin{bmatrix} -\vartheta I & -\xi^T(0) \\ * & -P \end{bmatrix} \leq 0. \tag{B.5}$$

$$\begin{aligned} \Phi_1 &= \begin{bmatrix} \tilde{A}^T P + P \tilde{A} + \lambda^2 \tilde{A}^T \tilde{W}_0^T \tilde{W}_0 \tilde{A} + \tilde{C}^T \tilde{C} & -P \tilde{E} - \lambda^2 \tilde{A}^T \tilde{W}_0^T \tilde{W}_0 \tilde{E} & P \tilde{B} + \lambda^2 \tilde{A}^T \tilde{W}_0^T \tilde{W}_0 \tilde{B} \\ * & \lambda^2 \tilde{E}^T \tilde{W}_0^T \tilde{W}_0 \tilde{E} - \lambda^2 I & -\lambda^2 \tilde{E}^T \tilde{W}_0^T \tilde{W}_0 \tilde{B} \\ * & * & \lambda^2 \tilde{B}^T \tilde{W}_0^T \tilde{W}_0 \tilde{B} - \gamma^2 I \end{bmatrix} \tag{A.4} \\ &\begin{bmatrix} \frac{1}{a} \tilde{A}^T P \tilde{A} + \frac{a^2 - b^2}{a} P + \tilde{A}^T P + P \tilde{A} + \lambda^2 \tilde{A}^T \tilde{W}_0^T \tilde{W}_0 \tilde{A} + \tilde{C}^T \tilde{C} & -P \tilde{E} - \lambda^2 \tilde{A}^T \tilde{W}_0^T \tilde{W}_0 \tilde{E} & P \tilde{B} + \lambda^2 \tilde{A}^T \tilde{W}_0^T \tilde{W}_0 \tilde{B} \\ * & \lambda^2 \tilde{E}^T \tilde{W}_0^T \tilde{W}_0 \tilde{E} - \lambda^2 I & -\lambda^2 \tilde{E}^T \tilde{W}_0^T \tilde{W}_0 \tilde{B} \\ * & * & \lambda^2 \tilde{B}^T \tilde{W}_0^T \tilde{W}_0 \tilde{B} - \gamma^2 I \end{bmatrix} < 0 \tag{A.5} \end{aligned}$$

Post- and pre-multiplying (B.5) by $diag(I, \Gamma_1)$ and its transpose, respectively, (B.5) can be written as (20). Thus, the input constraint can be satisfied.

REFERENCES

- [1] J. Singer and J. Bates, "U.S. Air Force, critic differ on XSS-11 mission objective," *Space News*, vol. 16, no. 15, p. 12, 2005.
- [2] M. Osborn, C. Clauss, B. Gorin, and C. Netwall, "Micro-satellite technology experiment (MiTeX) upper stage propulsion system development," in *Proc. 43rd AIAA/ASME/SAE/ASEE Joint Propuls. Conf. Exhib.*, Jul. 2007, p. 5434.
- [3] D. Li, Z. Zhu, R. Zhang, H. Chen, J. Zhang, and S. Wan, "The design and in-orbit test of the companion microsatellite attitude control system in SZ-7 flight mission," *J. Astronaut.*, vol. 32, no. 3, pp. 495–501, Mar. 2011.
- [4] J. D. Boskovic, S.-M. Li, and R. K. Mehra, "Globally stable adaptive tracking control design for spacecraft under input saturation," in *Proc. 38th IEEE Conf. Decis. Control*, vol. 2, Dec. 1999, pp. 1952–1957.
- [5] C.-D. Yang and Y.-P. Sun, "Mixed H_2/H_∞ state-feedback design for microsatellite attitude control," *Control Eng. Pract.*, vol. 10, no. 9, pp. 951–970, Sep. 2002.
- [6] Z. Zhu, Y. Xia, and M. Fu, "Adaptive sliding mode control for attitude stabilization with actuator saturation," *IEEE Trans. Ind. Electron.*, vol. 58, no. 10, pp. 4898–4907, Oct. 2011.
- [7] B. Xiao, Q. Hu, and Y. Zhang, "Adaptive sliding mode fault tolerant attitude tracking control for flexible spacecraft under actuator saturation," *IEEE Trans. Control Syst. Technol.*, vol. 20, no. 6, pp. 1605–1612, Nov. 2012.
- [8] X. Zhang, Q. Zong, B. Tian, and W. Liu, "Continuous robust fault-tolerant control and vibration suppression for flexible spacecraft without angular velocity," *Int. J. Robust Nonlinear Control*, vol. 29, no. 12, pp. 3915–3935, Aug. 2019.
- [9] X.-W. Huang and G.-R. Duan, "Robust control allocation in attitude fault-tolerant control for combined spacecraft under measurement uncertainty," *IEEE Access*, vol. 7, pp. 156191–156206, 2019.
- [10] Y.-C. Chak, R. Varatharajoo, and Y. Razoumny, "Disturbance observer-based fuzzy control for flexible spacecraft combined attitude & sun tracking system," *Acta Astronaut.*, vol. 133, pp. 302–310, Apr. 2017.
- [11] Z. Liu, J. Liu, and L. Wang, "Disturbance observer based attitude control for flexible spacecraft with input magnitude and rate constraints," *Aerosp. Sci. Technol.*, vol. 72, pp. 486–492, Jan. 2018.
- [12] L. Fan, H. Huang, L. Sun, and K. Zhou, "Robust attitude control for a rigid-flexible-rigid microsatellite with multiple uncertainties and input saturations," *Aerosp. Sci. Technol.*, vol. 95, Dec. 2019, Art. no. 105443.
- [13] G. Duan and T. Zhao, "Parametric output regulation using observer-based PI controllers with applications in flexible spacecraft attitude control," *Sci. China Inf. Sci.*, vol. 64, no. 7, Jul. 2021, Art. no. 172210.
- [14] J.-H. Huo, T. Meng, R.-T. Song, and Z.-H. Jin, "Adaptive prediction backstepping attitude control for liquid-filled micro-satellite with flexible appendages," *Acta Astronaut.*, vol. 152, pp. 557–566, Nov. 2018.
- [15] L. Xie and C. E. D. Souza, "Robust H_∞ control for linear systems with norm-bounded time-varying uncertainty," *IEEE Trans. Autom. Control*, vol. 37, no. 8, pp. 1188–1191, Aug. 1992.
- [16] Y. Jia, "Robust control with decoupling performance for steering and traction of 4WS vehicles under velocity-varying motion," *IEEE Trans. Control Syst. Technol.*, vol. 8, no. 3, pp. 554–569, May 2000.
- [17] C. Liu, F. Wang, K. Shi, X. Wang, and Z. Sun, "Robust H_∞ control for satellite attitude control system with uncertainties and additive perturbation," *Int. J. Sci.*, vol. 1, no. 2, pp. 1–9, 2014.
- [18] F. Lizarralde and J. T. Wen, "Attitude control without angular velocity measurement: A passivity approach," *IEEE Trans. Autom. Control*, vol. 41, no. 3, pp. 468–472, Mar. 1996.
- [19] B. Wu, X. Cao, and Z. Li, "Multi-objective output-feedback control for microsatellite attitude control: An LMI approach," *Acta Astronaut.*, vol. 64, nos. 11–12, pp. 1021–1031, Jun. 2009.
- [20] S. Wu and S. Wen, "Robust H_∞ output feedback control for attitude stabilization of a flexible spacecraft," *Nonlinear Dyn.*, vol. 84, no. 1, pp. 405–412, Apr. 2016.
- [21] S. Wu, W. Chu, X. Ma, G. Radice, and Z. Wu, "Multi-objective integrated robust H_∞ control for attitude tracking of a flexible spacecraft," *Acta Astronautica*, vol. 151, pp. 80–87, Oct. 2018.
- [22] X. Gao, K. L. Teo, and G.-R. Duan, "Non-fragile robust H_∞ control for uncertain spacecraft rendezvous system with pole and input constraints," *Int. J. Control*, vol. 85, no. 7, pp. 933–941, Jul. 2012.
- [23] G. Yang and J. Wang, "Non-fragile H_∞ control for linear systems with multiplicative controller gain variations," *Automatica*, vol. 37, no. 5, pp. 727–737, May 2001.
- [24] L. Li and Y. Jia, "Non-fragile dynamic output feedback control for linear systems with time-varying delay," *IET Control Theory Appl.*, vol. 3, no. 8, pp. 995–1005, Aug. 2009.
- [25] W. Che and Y. Wang, "Non-fragile dynamic output feedback H_∞ control for continuous-time systems with controller coefficient sensitivity consideration," in *Proc. 23rd IEEE Conf. Chin. Control Decis.*, May 2011, pp. 2441–2446.
- [26] K. Ma, G. Zhuang, H. Zhang, G. Zhao, Y. Lin, and J. Wang, "Improved non-fragile state feedback control for stochastic jump systems with uncertain parameters and mode-dependent time-varying delays," *IEEE Access*, vol. 8, pp. 97676–97688, 2020.
- [27] J. Zhang, J. Song, J. Li, F. Han, and H. Zhang, "Observer-based non-fragile H_∞ consensus control for multi-agent systems under deception attacks," *Int. J. Syst. Sci.*, vol. 52, no. 6, pp. 1223–1236, Apr. 2021.
- [28] C. Liu, Z. Sun, K. Shi, and F. Wang, "Robust dynamic output feedback control for attitude stabilization of spacecraft with nonlinear perturbations," *Aerosp. Sci. Technol.*, vol. 64, pp. 102–121, May 2017.
- [29] C. Liu, G. Vukovich, K. Shi, and Z. Sun, "Robust fault tolerant non-fragile H_∞ attitude control for spacecraft via stochastically intermediate observer," *Adv. Space Res.*, vol. 62, no. 9, pp. 2631–2648, Nov. 2018.
- [30] P. M. Tiwari, S. Janardhanan, and M. U. Nabi, "Rigid spacecraft attitude control using adaptive integral second order sliding mode," *Aerosp. Sci. Technol.*, vol. 42, pp. 50–57, Apr. 2015.
- [31] S. D. Gennaro, "Passive attitude control of flexible spacecraft from quaternion measurements," *J. Optim. Theory Appl.*, vol. 116, no. 1, pp. 41–60, Jan. 2003.
- [32] B. Wie, *Space Vehicle Dynamics and Control* (AIAA Education Series). Reston, VA, USA: AIAA, 1998.
- [33] R. Zhang, J. Qiao, T. Li, and L. Guo, "Robust fault-tolerant control for flexible spacecraft against partial actuator failures," *Nonlinear Dyn.*, vol. 76, no. 3, pp. 1753–1760, Jan. 2014.
- [34] J. Ackermann, *Sampled-Data Control Systems: Analysis and Synthesis, Robust System Design*. New York, NY, USA: Springer-Verlag, 1985.
- [35] L. Xie, "Output feedback H_∞ control of systems with parameter uncertainty," *Int. J. Control*, vol. 63, no. 4, pp. 741–750, Mar. 1996.
- [36] S. Huang and G. Yang, "Non-fragile H_∞ dynamic output feedback control for uncertain Takagi–Sugeno fuzzy systems with time-varying delay," *Int. J. Syst. Sci.*, vol. 47, no. 12, pp. 2954–2964, 2016.
- [37] C. Scherer, P. Gahinet, and M. Chilali, "Multiobjective output-feedback control via LMI optimization," *IEEE Trans. Autom. Control*, vol. 42, no. 7, pp. 896–911, Jul. 1997.
- [38] L. El-Ghaoui, E. Feron, and V. Balakrishnan, *Linear Matrix Inequalities in System and Control Theory*. Philadelphia, PA, USA: Society for Industrial and Applied Mathematics, 1994.
- [39] L. Zhao and Y. Jia, "Multi-objective output feedback control for autonomous spacecraft rendezvous," *J. Franklin Inst.*, vol. 351, no. 5, pp. 2804–2821, May 2014.
- [40] P. Gahinet, "Explicit controller formulas for LMI-based H_∞ synthesis," *Automatica*, vol. 32, no. 7, pp. 1007–1014, Jul. 1996.
- [41] Y. Jia, *Robust H_∞ Control*. Beijing, China: Science Press, 2007.



YI LI received the bachelor's degree from Shandong University, Jinan, China, in 2012. He is currently pursuing the Ph.D. degree in control theory and engineering with the School of Automation Science and Electrical Engineering, Beihang University.

His research interests include spacecraft attitude control and on-orbit capturing.

...